Matrix degradation in osteoarthritis primes the superficial region of cartilage for mechanical damage

Cooke, Megan E.; Lawless, Bernard M.; Jones, Simon W.; Grover, Liam M.

DOI:
10.1016/j.actbio.2018.07.037

Document Version
Publisher's PDF, also known as Version of record

Citation for published version (Harvard):
Cooke, ME, Lawless, BM, Jones, SW & Grover, LM 2018, 'Matrix degradation in osteoarthritis primes the superficial region of cartilage for mechanical damage', *Acta Biomaterialia*, vol. 78, pp. 320-328. https://doi.org/10.1016/j.actbio.2018.07.037

Acta Biomaterialia 78 (2018) 320–328

Contents lists available at ScienceDirect

Acta Biomaterialia

journal homepage: www.elsevier.com/locate/actabiomat

Full length article

Matrix degradation in osteoarthritis primes the superficial region of cartilage for mechanical damage

Megan E. Cooke [a,b,*], Bernard M. Lawless [c], Simon W. Jones [b], Liam M. Grover [a]

[a] School of Chemical Engineering, University of Birmingham, Birmingham, UK
[b] MRC ARUK Centre for Musculoskeletal Ageing, QE Hospital, University of Birmingham, Birmingham, UK
[c] Department of Mechanical Engineering, University of Birmingham, Birmingham, UK

ARTICLE INFO

Article history:
Received 21 February 2018
Received in revised form 23 June 2018
Accepted 17 July 2018
Available online 29 July 2018

Keywords:
Osteoarthritis
Viscoelastic
Dynamic mechanical analysis
Cartilage
Thermogravimetric analysis

ABSTRACT

Osteoarthritis (OA) is a degenerative disease that affects 25% of the world's population over fifty years of age. It is a chronic disease of the synovial joints, primarily the hip and knee. The main pathologies are degradation of the articular cartilage and changes to the subchondral bone, as a result of both mechanical wear and a locally elevated inflammatory state. This study compares the viscoelastic properties of cartilage that represents the biochemical changes in OA and age-matched healthy tissue. Further, the mechanical damage induced by this compressive loading cycle was characterised and the mechanism for it was investigated. The storage modulus of OA cartilage was shown to be significantly lower than that of healthy cartilage whilst having a higher capacity to hold water. Following mechanical testing, there was a significant increase in the surface roughness of OA cartilage. This change in surface structure occurred following a reduction in sulphated glycosaminoglycan content of the superficial region in OA, as seen by alcian blue staining and quantified by micro X-ray fluorescence. These findings are important in understanding how the chemical changes to cartilage matrix in OA influence its dynamic mechanical properties and structural integrity.

Statement of significance

Cartilage has a very specialised tissue structure which acts to resist compressive loading. In osteoarthritis (OA), there is both mechanically- and chemically-induced damage to cartilage, resulting in severe degradation of the tissue. In this study we have undertaken a detailed mechanical and chemical analysis of macroscopically undamaged OA and healthy cartilage tissue. We have demonstrated, for the first time in human tissue, that the mechanical degradation of the tissue is attributed to a chemical change across the structure. In macroscopically undamaged OA tissue, there is a reduction in the elastic response of cartilage tissue and an associated destabilisation of the matrix that leaves it susceptible to damage. Understanding this allows us to better understand the progression of OA to design better therapeutic interventions.

1. Introduction

In osteoarthritis (OA), a degenerative disease of synovial joints, there are both mechanical and inflammation-induced processes that result in changes to joint tissues [1–3]. Of these, the most commonly reported is degeneration of hyaline cartilage, whilst there are also pathological changes to the subchondral bone and synovium [4,5]. Cartilage is avascular and therefore has a limited capacity for self-repair, so structural damage to its surface is largely irreversible. It has three main non-water components: chondrocytes, a network of collagen type II (Col II), and proteoglycans. These proteoglycans bind water, which, in turn, makes up between 70–80% of cartilage by weight [6,7]. The distribution and alignment of these three constituents results in a graduated tissue structure which brings about distinct mechanical properties [8].

Mechanically, cartilage provides both a low-friction surface for articulation of the joint and acts to transmit compressive loading forces to the underlying subchondral bone. Similar to many other tissues in the body, it exhibits time-dependent viscous and elastic

* Corresponding author at: School of Chemical Engineering, University of Birmingham, Birmingham, UK
E-mail address: megan.cooke.research@gmail.com (M.E. Cooke).

https://doi.org/10.1016/j.actbio.2018.07.037
1742-7061/

behaviour in both compression and tension [9]. The superficial region consists of Col II fibres oriented parallel to the articulating surface giving local tensile strength. This collagen network becomes more disordered in the middle region and in the deep zone and through the tidemark, fibres are aligned perpendicular to the articulating surface. In OA, the Col II network deteriorates, starting from the articulating surface in early OA and progressing through the tissue with increasing OA severity, as measured by Hollander et al., using Mankin grading [10]. Aggrecan, the most common proteoglycan, is found primarily in the middle and deep zones. It is the second most abundant protein in cartilage following Col II and it sits along a hyaluronic acid backbone. Individual aggrecan molecules have sulphated glycosaminoglycan (sGAG) chains (keratan and chondroitin sulphate) coming from the aggrecan core protein that form a bottle-brush structure. These sGAG chains have a negative charge resulting in a high binding affinity to water.

The binding of water to proteoglycans is partly responsible for the compressive mechanical properties of cartilage. The carboxyl and sulphate groups of chondroitin sulphate and sulphate group of keratan sulphate provide fixed charge density (FCD) to the tissue, which, in combination with repulsion between neighbouring negatively charged chains results in a high osmotic pressure [11]. In healthy cartilage this pressure is compensated by the Col II network which restricts over-swelling and allows the tissue to resist compressive forces [11]. In OA an increase in matrix metalloproteins (MMPs) and aggrecanases, particularly members of the ADAMTS (A Disintegrin and Metalloproteinase with Thrombospondin motifs) family, have been identified as primary factors in the catabolism of articular cartilage matrix proteins including aggrecan and Col II [2,10]. Changes in these matrix components have been shown to affect the mechanical properties of human cartilage [12] and the dynamic mechanical properties of canine tissue with destabilisation-induced OA [13].

The viscoelastic properties of a material can be quantified by numerous methods including creep, stress relaxation and dynamic mechanical analysis (DMA). Unlike creep and stress relaxation which usually have long time constants, DMA is a dynamic testing method. By applying an oscillating force to a specimen and analysis of the out-of-phase displacement response, the frequency-dependent storage and loss moduli can be calculated. The storage modulus (E') describes a material's ability to store energy for elastic recoil while the loss modulus (E'') characterises the material's ability to dissipate energy [14]. Studies have examined articular cartilage at low strain rates [15,16] and others have used DMA to assess frequency-dependency of the viscoelastic properties of cartilage in bovine and human specimens [17]. However, the effects of OA on the viscoelastic properties of human cartilage have so far only been examined using indentation methods and these looked at femoral head cartilage, where the direction and magnitude of loading is harder to define [18].

Changes to both the mechanical and physicochemical properties of cartilage are of interest in osteoarthritis, and physical techniques for tissue analysis are becoming more commonly utilised. As such, quantitative mapping of chemical elements present in tissues is now possible using micro X-ray fluorescence. This gives good spatial resolution of elements and has been used in a number of tissues including cartilage [19–21]. Other quantitative techniques that are traditionally used in materials science but not biological analysis such as thermogravimetric analysis are also being transferred to understand the chemical structure of tissues and biomaterials. Cartilage is interesting thermogravimetrically due to its high water content, and such, the changes in hydration in different disease states and from different anatomical locations are interesting when considering the importance of water on the inherent mechanical properties of cartilage [22]. In OA, there is an observed change in the joint surface as cartilage becomes fibrillated. Interferometry is a commonly used technique in the analysis of surfaces but as yet its use in characterising biological surfaces is infrequent. These techniques can all be used to enhance knowledge and understanding of biological tissues.

Varus knee alignment as measured by the femorotibial angle has been shown to be a key factor for development and progression of OA [23]. In this position, the medial aspect of the knee joint experiences more damaging mechanical loading, as seen by a larger reduction in cartilage thickness [24]. However, the local inflammatory environment affects both aspects of the joint equally as the synovial fluid fills the joint space. In this study we have used human cartilage from the lateral aspect of the femoral condyles (Fig. 1) of OA subjects. This tissue is exposed to the same chemical environment but is macroscopically undamaged. As yet, no one has studied the links between the early mechanical and chemical changes to human OA cartilage. Therefore, the aim of this study was to determine the dynamic mechanical properties at a range of physiological frequencies and undertake a detailed chemical analysis to understand the differences observed in early, less structurally degraded, OA and healthy cartilage from the same anatomical region.

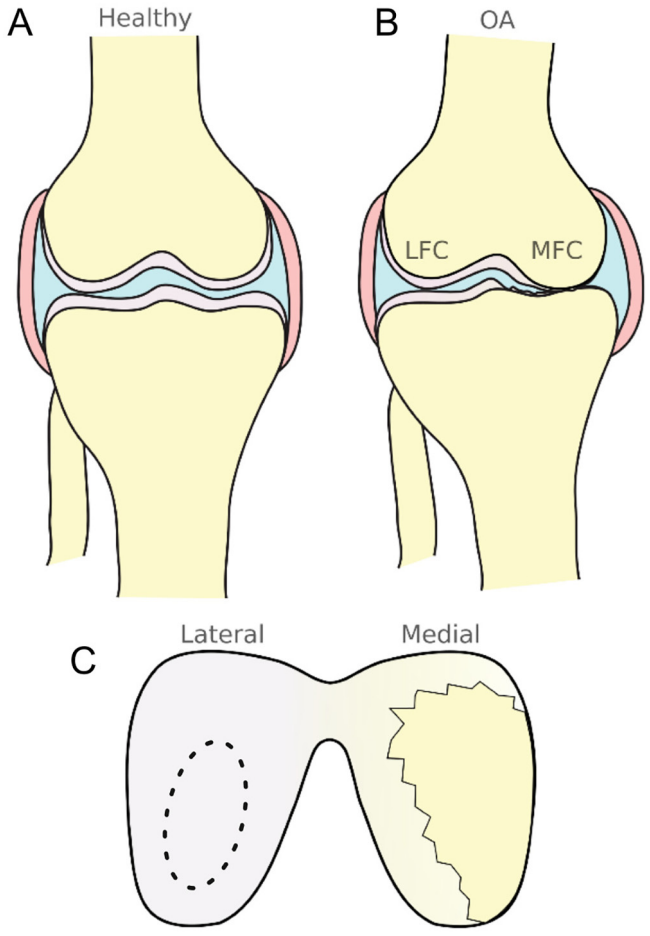

Fig. 1. Representation of healthy (A) and OA (B,C) joint structures. Varus loading in OA causes a reduced joint space in the medial aspect such that cartilage of the medial aspect including the medial femoral condyle (MFC) undergoes severe mechanical degradation, revealing the underlying subchondral bone. The lateral aspect of the joint maintains a wider joint spacing such that tissue of the lateral femoral condyle (LFC) experiences less mechanical damage. The dashed region in C indicates where cartilage explants were taken for this study.

2. Methods

2.1. Materials

All materials listed below were supplied by Sigma Aldrich, Gillingham, UK unless otherwise stated.

2.2. Tissue source and preparation

OA tissue was donated by consenting patients following elective total knee replacement and was approved by the United Kingdom National Research Ethics Service (Nottingham Research Ethics Committee 1 (05/Q2403/24)). Ethical approval was also obtained (Derby Research Ethics Committee 1 (11/H0405/2)) to collect non-OA knee cartilage from post mortem donors (mean ± SEM age: 74 ± 5 years) (Kings Mill Hospital, Sutton in Ashfield, UK) with no history of joint pain or evidence of cartilage fibrillation based on chondropathy assessment. Consent was obtained from all patients or their families.

Medial patellofemoral OA was diagnosed radiographically, by a narrowing of the joint space; healthy tissue was donated post mortem by patients with no history of joint disease and with no gross evidence of OA. 22 healthy cartilage explants were taken from 6 subjects and 37 OA explants were taken from 14 subjects; further details are shown in Table 1.

Full thickness cartilage was excised from the underlying subchondral bone of the lateral femoral condyle using a scalpel, as indicated by the dashed region in Fig. 1. This region has been shown to be less mechanically loaded in OA than the medial side [25]. Cylindrical cartilage explants of 5.2 mm diameter were then produced using a cork borer. Each specimen underwent one freeze–thaw cycle; freezing and thawing has been shown to not alter the dynamic properties of cartilage [26].

2.3. Dynamic mechanical analysis (DMA)

The viscoelastic properties of healthy and OA specimens were quantified using a Bose ElectroForce 3200 testing machine and the accompanying Bose WinTest 4.1 DMA software (TA Instruments, New Castle, DE, USA). Prior to testing, cartilage specimens were fully hydrated in Ringer's solution for 30 min before being removed from the solution for testing. Cartilage specimens were placed on an aluminium base plate and were loaded using a 20 mm cylindrical compression platen that made contact with the articulating surface. Similar to previous cartilage studies, a sinusoidal compressive force of 16 to 36 N was applied to each specimen [27–30]. As the cartilage specimens were 5.2 mm in diameter, the peak load of 36 N induced a peak stress of 1.7 MPa which is similar to the estimated physiological peak stress during walking [31]. The mean applied stress was 1.22 MPa and the amplitude of applied stress was 0.95 MPa; the applied strain was 1.8–4.8% depending on specimen thickness. Before applying a frequency sweep, each specimen was preloaded to 3 N (to avoid initial slipping) and subjected to two preconditioning cycles. 1500 and 3000 cycles at 25 and 50 Hz respectively were applied, with 60 s between them, to achieve a dynamic 'steady-state' which has been stated to occur after around 1200 to 4500 preconditioning cycles for *ex vivo* cartilage [27,32,33]. The shift in mean level of displacement following these cycles is shown in Appendix Fig. A.8A as some excess fluid was removed. Following preconditioning, eight different physiologically-relevant sinusoidal frequencies (1, 8, 10, 12, 29, 49, 71 and 88 Hz for 17, 61, 73, 85, 190, 314, 450 and 555 cycles respectively) were applied to each cartilage specimen in order of increasing frequency [27]. The total testing time for each specimen was limited to 6 min and 35 s to reduce dehydration of the samples. For each frequency, the WinTest DMA software performed Fourier analyses of the sinusoidal force and displacement waves. From this analysis, the magnitudes of the load (F^*) and displacement (d^*), the phase lag (δ) and the frequency were quantified [32,34]. The viscoelastic properties, complex stiffness (k^*), storage stiffness (k') and loss stiffness (k'') were then calculated using:

$$k^* = \frac{F^*}{d^*} \tag{1}$$

$$k' = k^* cos\delta \tag{2}$$

$$k'' = k^* sin\delta \tag{3}$$

The storage (E') and loss (E'') moduli were then calculated, using a shape factor (SF)

$$SF = \frac{\pi d^2}{4t} \tag{4}$$

$$E' = \frac{k'}{SF} \tag{5}$$

$$E'' = \frac{k''}{SF} \tag{6}$$

For Eq. (4), d) is the specimen diameter (5.2 mm) and (t) is the specimen thickness which was measured as below.

2.4. Cartilage thickness

The thickness of each cartilage specimen was measured using a needle thickness test following DMA. Briefly, a sharp needle was attached to the machine's displacement transducer (1 μm resolution) and the needle was pushed through the full thickness of the cartilage specimen. Further details of this technique are described elsewhere [35].

2.5. Thermogravimetric analysis

The mass change relating to water loss in healthy and OA cartilage samples was measured using thermogravimetric analysis (TGA) in air. Cartilage explants were heated from 25–250 °C at a rate of 1 K.min^{-1} and gas flow rate of 30 ml.min^{-1} using a TG209 F1 (Netzsch, Germany) in aluminium oxide crucibles with lids (Netzsch, Germany). A background correction of the crucible environment was performed prior to testing cartilage samples. The mass was measured continually during heating and the change in mass plotted; the rate of mass change was calculated by the accompanying Netzsh TA4 software (Netzsch, Germany).

2.6. Micro-X-ray fluorescence (μXRF)

Elemental maps of cartilage sections were generated using a M4 Tornado μXRF system and accompanying M4 software (Bruker Nano Gmbh, Berlin, Germany). 30 μm cartilage sections were mapped with a pixel size of 20 μm and scanning at 100 ms/px under vacuum of 200 mbar. The distribution of sulphur was imaged and quantified in different regions of OA and healthy

Table 1
Age and genders of the 20 patients whose cartilage was studied, n (explants) corresponds to specimens used for DMA.

Tissue	n (explants)	Age	Gender	Thickness (mm)
Healthy	6 (22)	76 (53–87)	M = 3	1.465 ± 0.240
OA	14 (37)	71 (56–81)	M = 10	1.463 ± 0.206

cartilage without and with mechanical testing protocols applied to it. Absolute quantification was used to compare sulphur content between samples; relative quantification was used to visualise calcium, phosphorus and sulphur content (M4 software).

2.7. Tissue sectioning and histology

Sections were snap-frozen in liquid nitrogen and embedded in TissueTek OCT (optimal cutting temperature) compound (Sakura, Finetek, Torrance, CA, USA) for sectioning using an OFT5000 cryostat (Bright Instruments Ltd, Luton, UK). 10 μm sections were fixed to slides and kept at −20 °C until staining. OCT was washed twice with dH_2O before an alcian blue working solution of (in 3% acetic acid) was added for 10 min. Following staining, sections were dehydrated using 50, 70, 90, 95 and 100% ethanol before clearing with xylene and mounting with DPX (distyrene, plasticiser and xylene) resin (Honeywell-Fluka, NJ, US).

2.8. Interferometry

A MicroXAM Interferometer (KLA Tencor, UK) was used to map and quantify surface roughness of healthy and OA cartilage explants both untested and after DMA testing. For each 5.2 mm diameter cartilage explant, 9 216 x 198 nm regions were imaged, stitched and areal surface roughness (Sa) was calculated using Scanning Probe Image Processor software (Image Metrology, Denmark).

2.9. Data analysis and statistical methods

Statistical analysis was performed using Prism 7 (GraphPad, CA, USA). Two-way ANOVA with Tukey's post hoc testing for multiple comparisons was used for mechanical data. Student's t-tests were used to compare differences between healthy and OA tissues, and also between samples tested and untested by DMA. Results where $p < 0.05$ were considered significant. Logarithmic frequency dependent behaviour was described by Eqs. (7) and (8), where (f) refers to frequency.

$$E' = Aln(f) + B \tag{7}$$

$$E'' = Cln(f) + D \tag{8}$$

3. Results

3.1. Viscoelastic properties of healthy and OA specimens

The frequency dependence of the storage (E') and loss (E'') moduli are shown in Figs. 2A and 2B for healthy and OA cartilage respectively. The storage modulus of both healthy and OA cartilage was logarithmically frequency dependent and the behaviour plateaued from around 50 Hz (Fig. 2A). Results of two-way ANOVA/Tukey showed that in both the loss and storage modulus, there were significant effects of frequency ($p < 0.001$), the effects of disease in relation to frequency were significant in the storage modulus ($p < 0.001$) but not in the loss modulus ($p = 0.002$). Students t-tests of the mean moduli values showed that the storage modulus of healthy cartilage was significantly higher ($p < 0.05$) than that of OA cartilage at all frequencies with the exception of 88 Hz ($p = 0.058$), as shown in Appendix Table A.4. The loss moduli were also logarithmically frequency dependent and plateaued around 50 Hz. Table 2 shows the values which satisfy Eqs. (7) and (8) for both E' and E''; the viscoelastic behaviour was found to be linearly logarithmic. The area inside the hysteresis loops (Fig. 3) was greater for OA specimens than healthy, at both low and high

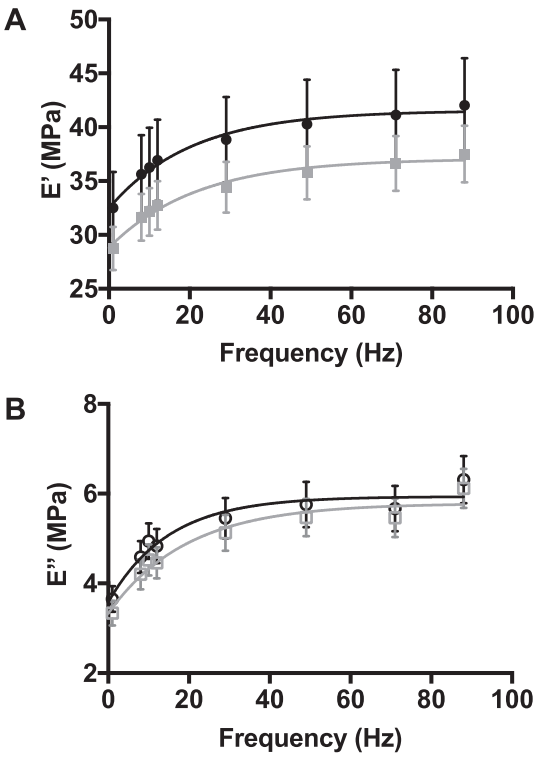

Fig. 2. A) Storage modulus (E') of healthy (•) and OA (■) cartilage with 95% confidence intervals, B) Loss modulus (E'') of healthy (○) and OA (□) cartilage with 95% confidence intervals; H n = 22, OA n = 37.

frequencies, indicating that the healthy specimens had a more elastic response. The mean level of displacement was fairly stable throughout testing (Appendix Fig. A.8B).

3.2. Thermogravimetric analysis of OA and healthy cartilage

The binding of water by the proteoglycan network provides a large contribution to the compressive properties of articular cartilage, so to elucidate the changes seen in Fig. 2, the amount of water in these samples was accurately measured. TGA was used to quantify the amount of bound water in untested and post-DMA cartilage explants from both healthy and OA subjects. Fig. 4A shows the change in % mass of OA and healthy cartilage between 25–250 °C. Between these temperatures, the loss of water was seen up to around 90 °C and a further transition started at around 210 °C. The linear region of water loss as shown in Table 3 resulted in a larger change in mass between the healthy and OA specimens (Fig. 4B). The OA samples showed a significantly larger change in mass by 100°C ($p < 0.05$) and a faster peak rate of mass change, as seen by the DTG curve (dashed line). The further change in mass to 250 °C was very similar between the healthy and OA samples, −23.76 and −23.08% respectively.

3.3. Mapping and quantification of sulphur in cartilage sections

μXRF was used to quantify the changes in aggrecan distribution in OA and healthy tissue by measuring the levels of sulphur across cartilage sections. Fig. 5 shows that in untested samples, healthy cartilage had a consistent gradient across the tissue where sulphur was most abundant in the deep zone and less so in the superficial region. OA cartilage, however, had a less regular gradient towards the surface and visually the superficial region showed minor damage to the surface even in untested samples. Following DMA, the surface of healthy cartilage was slightly deformed along the

Table 2
Storage and loss modulus coefficients as Eqs. (7) and (8) from regression analyses. All coefficients and constants values are MPa, $p < 0.05$ indicates that the logarithmic regression was significant.

Sample	Property	A	B	C	D	R^2	P
Healthy	E′	2.155	31.79	–	–	0.977	<0.05
OA	E′	1.968	28.07	–	–	0.977	<0.05
Healthy	E″	–	–	0.551	3.576	0.961	<0.05
OA	E″	–	–	0.585	3.166	0.956	<0.05

normal direction of collagen fibril alignment in this region. However, the surface was not macroscopically ruptured as seen in the OA samples. The OA cartilage had severe damage to the articulating surface post-DMA, while the middle and deep regions retained their structure. Fig. 5B shows the relative quantification of sulphur distribution across the sections. Healthy and OA sections had similar sulphur levels in the deep and middle zones, but the OA samples had lower levels in the superficial zone. Quantification of the post-DMA samples shows that in both OA and healthy samples, mechanical testing reduced the sulphur content, which is likely due to changes in aggrecan proteoglycan organisation. However, this change was more marked in the superficial region of OA samples compared to healthy. Quantification of the OA samples post-DMA was limited at the articulating surface due to the mechanically-induced damage. In Fig. 5C, co-localisation of calcium and phosphorus was evidence of mineral deposits in the cartilage. These were observed in the OA but not healthy cartilage samples.

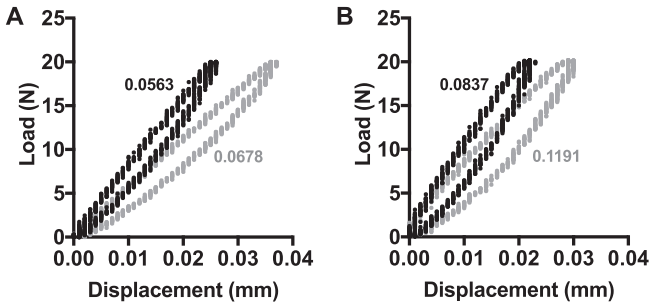

Fig. 3. Hysteresis loops of healthy (black) and OA(grey) cartilage at A)10 Hz and B) 88 Hz, inset values of hysteresis area (Nmm).

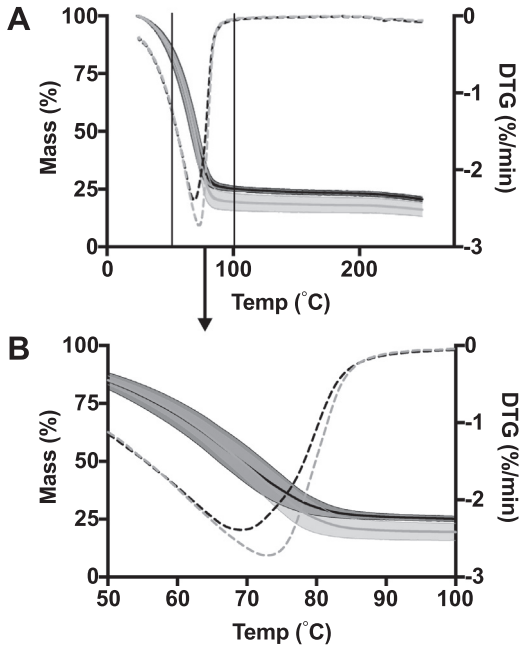

Fig. 4. Thermogravimetric analysis of OA (grey) and healthy (black) cartilage between (A) 20–250 °C. Dashed line indicates kinetics of mass change (DTG). Inset (B) shows the end of the water loss region.

3.4. Histological staining

Whilst μXRF was useful for quantifying the changes in element distribution, the resolution was limited. Therefore, in order to better visualise both the proteoglycan distribution and physical changes to the superficial region, alcian blue staining of 10 μm cartilage sections was performed. In healthy cartilage (Fig. 6A-C), there was a gradient of proteoglycan, with the heaviest staining in the deep region and getting progressively lighter towards the superficial region. Following DMA of healthy cartilage, there was no visible difference in the surface structure (Fig. 6C) from the untested sample (Fig. 6A) In OA cartilage, the distribution of proteoglycan was less ordered and there was evidence of cell clusters. Further, although there was a gradient, there were also regions of darker staining throughout the middle region (Fig. 6D). Compared to the healthy tissue, the staining was less even. There were large cracks visible in the surface with fragments of tissue detaching from the section (Fig. 6E, F).

3.5. Articulating surface damage

Following DMA, the surface region of OA cartilage samples was visibly damaged, and it was also seen in histological sections (Fig. 6). To quantify the damage, interferometry was used to measure surface roughness. Fig. 7A shows that there was no difference between healthy specimens that have and have not undergone a dynamic testing protocol. In the OA samples (Fig. 7B), the surface roughness prior to testing was significantly higher than that of the healthy samples ($p < 0.05$) indicating an initial degree of mechanical damage that was not macroscopically visible. Following DMA, the surface roughness of OA specimens was significantly higher than subject-matched samples that have not undergone DMA ($p < 0.05$).

Table 3
TG parameters of healthy and OA samples during linear water loss transition.

Sample (N)	Linear region (°C)	DTG peak (°C)	DTG peak (%/min)	Linear region mass change
Healthy (4)	52.30–78.50	69.71	−2.39	−54.22%
OA (4)	53.58–79.99	71.87	−2.74	−60.87%

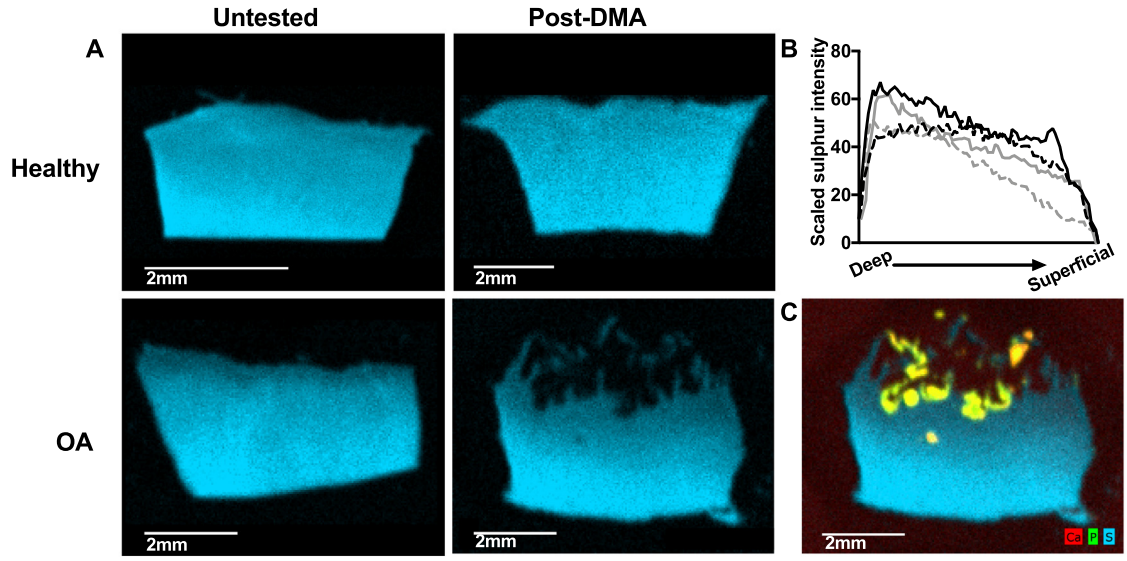

Fig. 5. A) μXRF mapping of distribution of sulphur in cartilage sections, highest intensity depicted by brighter colour closest to the bone interface at the bottom of each image. B) Quantification of sulphur across healthy (black) and OA (grey) cartilage sections that are untested (solid) and post-DMA (dashed) (n = 3). C) Sulphur, calcium and phosphorus map showing evidence of Ca and P localisation in mineral deposits.

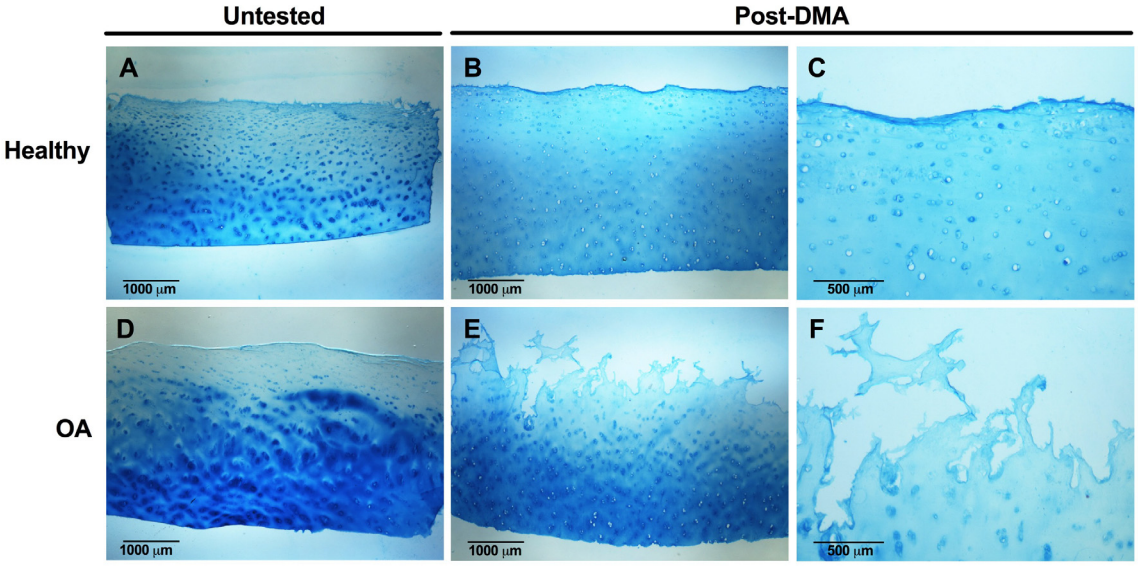

Fig. 6. Representative alcian blue staining of 10 μm thick cartilage sections from healthy (A-C) and OA (D-F) samples both untested (A, D) and post-DMA (B&C, E&F). The radial gradient observed in the lower magnification images is an artefact of the light microscope used to image these sections.

4. Discussion

This study aimed to understand the differences in frequency-dependent viscoelastic properties of isolated healthy and OA human articular cartilage and compare these to the physicochemical changes seen. Tissue was excised from the lateral aspect of the OA joint, which is known to be less exposed to mechanical stresses than the medial aspect, and thus was used to represent cartilage which was not excessively mechanically loaded but was exposed to the same chemical environment.

The first component of this study determined the viscoelastic properties of healthy and OA human cartilage. The logarithmic frequency-dependent behaviour in both the storage and loss modulus was similar to findings in human and bovine cartilage [17,29,30]. The significant reduction in storage modulus across a range of frequencies in OA specimens is likely to be indicative of disruption to the matrix structure as a result of OA cytokines, MMPs and altered joint loading. The solid matrix components of cartilage, Coll II and the aggrecan-rich proteoglycan network, are primarily responsible for the compressive stiffness of cartilage and was shown to be reduced in OA. This difference was statistically significant at all but the highest frequency, 88 Hz ($P = 0.0581$), which has previously been implicated as a frequency brought about during a rapid heel strike rise time that may predispose subjects to OA [27,36]. The storage and loss moduli of healthy femoral condyle cartilage were similar to that of 'healthy' human femoral head cartilage (obtained from subjects who had experienced a traumatic fracture of the femoral neck) and follow the same logarithmic trends [29]. The viscoelastic response in cartilage is caused by a combination of fluid flux and polymer chain

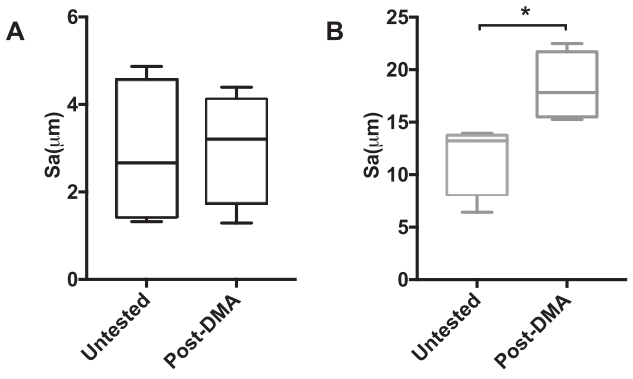

Fig. 7. Surface roughness of A) healthy and B) OA cartilage samples with or without DMA testing; $^{*}p < 0.05$.

sliding. The linear log trends seen in both moduli suggest that the compressive viscoelastic response may be dominated by the solid matrix components involved in polymer chain sliding.

Cartilage is comprised of more than 70% water, and the binding of water to proteoglycans provides high osmotic pressure, which is a key factor in the compressive properties of the tissue [11]. Therefore, the amount of water in each sample was measured by measuring the change in mass as a function of temperature. The higher water content of OA cartilage compared to healthy was shown thermogravimetrically by Sohar et al. [22]. However, their study showed the end of the water TG step at higher temperatures than seen in this study (102.25 °C and 104.60 °C compared to 78.50 °C and 79.99 °C for healthy and OA tissue respectively), which is likely due to the faster rate of heating used in their study (5 $K.min^{-1}$). The increased water content in OA samples is a result of an increased ability for the tissue to swell. This change in swelling capacity is due to breakdown of the Col II network associated with matrix catabolism in OA as measured by Bank et al. They found that an increased swelling percentage correlated with an increased percentage of degraded collagen in human samples from OA femoral head cartilage [37]. This reduces the elastic restraint on the tissue, meaning more extrafibrillar water can be held [22,38]. Cartilage swelling as a result of changes to the matrix composition has been shown previously using delayed gadolinium enhanced magnetic resonance imaging (dGEMRI), where a correlation between increased cartilage thickness and decreased GAG content was shown in the medial compartment of the knee [39]. The increased water content observed in OA samples may contribute to the similarities in loss modulus seen between healthy and OA tissue. The peak rate of mass change in the water TG step was higher in the OA samples and the peak was shifted to a higher temperature. The faster peak mass change was likely due to the increased water content, whilst the shifted peak suggests a higher binding strength of water to the PG network.

The gradient distribution of matrix components Col II and aggrecan are known to be critical to the proper mechanical functioning of cartilage. As water and its binding to PG is so important in the load-bearing capacity of cartilage, the distribution of the PG network was mapped. Benchtop μXRF was used to elementally map cartilage sections and was a simple and effective way to quantify the differences in sulphur content, corresponding to sGAG and aggrecan content in tissue samples. It is well known that the GAG content at the superficial region is lower than that of the middle and deep zones [40]. Here, however, seen by less bright pixels and quantified by line gradients from the deep to superficial zones, we saw a further reduction in the superficial region in OA cartilage. The reason for this may be proximity and contact with the synovial fluid, which, in the inflamed state of OA has a higher concentration of catabolic MMPs and cytokines [1]. Further, the identification of mineral-like deposits near the cartilage surface of OA cartilage suggested that mineralisation in OA may occur prior to visible mechanical damage to the superficial region. Tissue mineralisation of cartilage and meniscus are common in end-stage OA, usually seen as deposits of hydroxyapatite (HAp) and calcium pyrophosphate dihydrate (CPPD) crystals [41].

These mineral deposits were seen primarily in the upper middle and superficial regions of the cartilage sections; they may have a role in the observed surface damage following DMA. Relatively large (they can be seen radiographically), hard particles in a soft tissue could act as stress concentrations for cracks in cartilage to form, similar to the cracks that form following a traumatic insult to the cartilage surface [42]. Measuring the changes in surface roughness was achieved using interferometry, a technique commonly used in electronics for profiling surfaces. It enabled the quantification of the surface damage by analysing the peaks and valleys using light reflectance to quantify surface roughness. The significant increase in surface roughness following DMA in the OA subjects indicated that the superficial region was more susceptible to damage as has been shown previously in bovine tissue [43,44]. Further, the difference in Sa between healthy and OA samples observed was similar to the profile surface roughness (Ra) seen by Graindorge et al. between healthy (Ra = 1.06) and emery-roughened (Ra = 23.2) samples [45]. Whilst there was evidence of deformation of the superficial region of healthy tissue under μXRF, the superficial region of OA cartilage showed severe rupturing of the cartilage surface. Disruption to the matrix composition was likely responsible for this; as mentioned, there is a change in the collagen network originating at the articulating surface [10,46,47]. This reduces the tensile strength of the cartilage surface which reduces its ability to resist deformation.

Age-related changes to the proteoglycan content of the superficial layer of cartilage have been identified previously [11]. This effect is enhanced when the biochemical balance shifts in states such as trauma and OA causing increases in cytokines such as interleukin-1 (IL-1) and tumour necrosis factor alpha (TNFa) which drive matrix catabolism. Guilak et al. discuss the interplay between how physiological joint loading has protective mechanisms for regulating cytokine levels [48–50]. This balance between protective and damaging joint loading is likely key in the progression of OA. Another factor shown to increase the severity of OA symptoms is obesity; the increased loading on the joints due to higher body mass in combination with elevated production of adipose-derived cytokines (adipokines) [51]. These adipokines have been shown to increase production of many pro-inflammatory cytokines. Leptin, a well characterised adipokine, is increased in OA synovial fluid and has been shown to increase MMP-1 and MMP-13 production in human primary chondrocytes and to mediate greater IL-6 secretion from OA synovial fibroblasts [1,52]. Importantly in this study, while the joint loading of the OA subjects is focused in the medial compartment of the joint, the use of tissue from the lateral compartment demonstrates the important effects of the inflammatory OA environment on cartilage tissue.

Limitations: The use of human tissue samples is limiting in the number available, particularly the numbers of post mortem samples. Firstly, this means that following a power analysis, an effect size of 0.31 should be expected for the presented number of samples and an effect size of 0.48 for the 22 patients that samples were retrieved from. Secondly, due to the limited number of human samples, the testing protocols for DMA were all performed in the same order, so the loading history may affect the viscoelastic measurements. Future studies could investigate whether the loading history affects the viscoelastic response by randomising the order of frequencies during testing. Further, as the cartilage surface is semi-translucent, white light interferometry values are solely relative to surfaces with similar optical properties to cartilage.

5. Conclusions

For the first time, we have linked the local changes in chemistry and structure to the dynamic mechanical properties of OA and healthy cartilage, isolated from the same anatomical region in human donors. There is a significant reduction in the storage moduli of cartilage from OA compared to age-matched healthy subjects, indicating that in OA the elastic response of cartilage deteriorates. This reduction in storage modulus was found to be likely due to a disruption to the collagen network as OA tissues showed a higher capacity to swell and bind water. Visible changes to the cartilage surface following DMA were investigated and an increased surface roughness was observed in osteoarthritic but not healthy tissue. Finally, the mechanism for this disruption was investigated using histological staining and μXRF mapping to determine and quantify the proteoglycan distribution in both healthy and OA tissue.

Acknowledgements

MEC gratefully acknowledges funding from the EPSRC Sci-Phy-4-Health Centre for Doctoral Training (EP/ L016346/1); DMA equipment used in this study was funded by Arthritis Research UK (Grant No. H0671). OA tissue was obtained with the help of Prof Ed Davis (Royal Orthopaedic Hospital, Birmingham). The post mortem tissue was obtained with the help of Prof David Walsh (University of Nottingham) and Deborah Wilson (Kings Mill Hospital, Sutton in Ashfield, Nottingham). The authors would like to thank Hamid Sadeghi for assistance during experimentation and Daniel M. Espino for discussion on aspects of this study.

Appendix A

Table A.4
Storage Modulus mean ± SD and *p*-values.

Frequency (Hz)	Healthy n = 22	OA n = 37	p
1	32.50 ± 1.60	28.74 ± 0.98	0.039
8	35.63 ± 1.74	31.63 ± 1.08	0.043
10	36.26 ± 1.77	32.13 ± 1.09	0.040
12	36.93 ± 1.82	32.74 ± 1.11	0.041
29	38.84 ± 1.91	34.42 ± 1.16	0.040
49	40.29 ± 1.99	35.76 ± 1.21	0.043
71	41.13 ± 2.01	36.63 ± 1.25	0.050
88	42.03 ± 2.10	37.52 ± 1.30	0.058

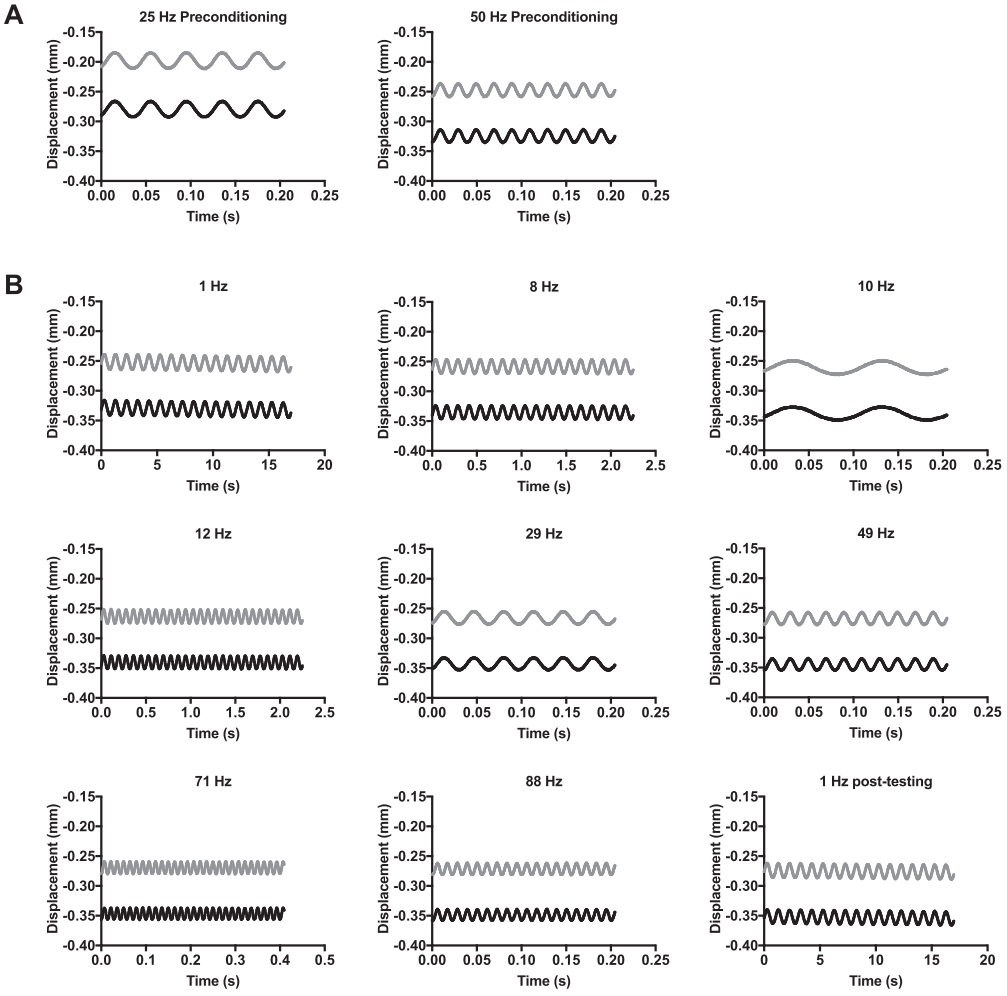

Fig. A.8. Temporal displacement of OA (grey) and healthy (black) cartilage during A) preconditioning cycles and B) testing frequencies. For a representative healthy specimen, the displacement amplitude for 1 Hz at the beginning of cycling was 0.025 mm and for 1 Hz at the end of the testing was 0.022 mm. In this OA specimen, the displacement amplitude for 1 Hz was 0.024 mm at both the start and end of the testing protocol.

References

[1] A.M. Philp, E.T. Davis, S.W. Jones, Developing anti-inflammatory therapeutics for patients with osteoarthritis, Rheumatology (Oxford, England) 56 (2017) 869–891.
[2] B. Caterson, C.R. Flannery, C.E. Hughes, C.B. Little, Mechanisms involved in cartilage proteoglycan catabolism, Matrix Biol. 19 (2000) 333–344.
[3] S.W. Jones, S.M. Brockbank, K.M. Clements, N. Le Good, D. Campbell, S.J. Read, M.R. Needham, P. Newham, Mitogen-activated protein kinase-activated protein kinase 2 (MK2) modulates key biological pathways associated with OA disease pathology, Osteoarthritis Cartilage 17 (2009) 124–131.
[4] M.B. Goldring, M. Otero, Inflammation in osteoarthritis, Curr. Opin. Rheumatol. 23 (2011) 471–478.
[5] D.P. Tonge, M.J. Pearson, S.W. Jones, The hallmarks of osteoarthritis and the potential to develop personalised disease-modifying pharmacological therapeutics, Osteoarthritis Cartilage 22 (2014) 609–621.
[6] A.J. Sophia Fox, A. Bedi, S.A. Rodeo, The basic science of articular cartilage: structure, composition, and function, Sports Health 1 (2009) 461–468.
[7] D.A. Reiter, R.A. Roque, P.-C. Lin, O. Irrechukwu, S. Doty, D.L. Longo, N. Pleshko, R.G. Spencer, Mapping proteoglycan-bound water in cartilage: Improved specificity of matrix assessment using multiexponential transverse relaxation analysis, Magn. Reson. Med. 65 (2011) 377–384.
[8] M.B. Goldring, S.R. Goldring, Articular cartilage and subchondral bone in the pathogenesis of osteoarthritis, Ann. N.Y. Acad. Sci. 1192 (2010) 230–237.
[9] S. Park, G.A. Ateshian, Dynamic response of immature bovine articular cartilage in tension and compression, and nonlinear viscoelastic modeling of the tensile response, J. Biomech. Eng. 128 (2006) 623–630.
[10] A.P. Hollander, I. Pidoux, A. Reiner, C. Rorabeck, R. Bourne, A.R. Poole, Damage to type II collagen in aging and osteoarthritis starts at the articular surface, originates around chondrocytes, and extends into the cartilage with progressive degeneration, J. Clin. Invest. 96 (1995) 2859–2869.
[11] E. Han, S.S. Chen, S.M. Klisch, R.L. Sah, Contribution of proteoglycan osmotic swelling pressure to the compressive properties of articular cartilage, Biophys. J . 101 (2011) 916–924.
[12] D.L. Robinson, M.E. Kersh, N.C. Walsh, D.C. Ackland, R.N. de Steiger, M.G. Pandy, Mechanical properties of normal and osteoarthritic human articular cartilage, J. Mech. Behav. Biomed. Mater. 61 (2016) 96–109.
[13] F. Guilak, A. Ratcliffe, N. Lane, M.P. Rosenwasser, V.C. Mow, Mechanical and biochemical changes in the superficial zone of articular cartilage in canine experimental osteoarthritis, J. Orthop. Res. 12 (1994) 474–484.
[14] K.P. Menard, Dynamic Mechanical Analysis: A Practical Introduction, CRC Press, second ed., Taylor & Francis Group, Boca Raton, 2008.
[15] J.S. Jurvelin, M.D. Buschmann, E.B. Hunziker, Mechanical anisotropy of human knee articular cartilage in compression, Trans. Orthop. Res. Soc. 217 (1996) 215–219.
[16] J.M. Fick, How the structural integrity of the matrix can influence the microstructural response of articular cartilage to compression, Connective Tissue Res. 54 (2013) 83–93.
[17] B.M. Lawless, H. Sadeghi, D.K. Temple, H. Dhaliwal, D.M. Espino, D.W.L. Hukins, Viscoelasticity of articular cartilage: analysing the effect of induced stress and the restraint of bone in a dynamic environment, J. Mech. Behav. Biomed. Mater. 75 (2017) 293–301.
[18] F. Richard, M. Villars, S. Thibaud, Viscoelastic modeling and quantitative experimental characterization of normal and osteoarthritic human articular cartilage using indentation, J. Mech. Behav. Biomed. Mater. 24 (2013) 41–52.
[19] P.M. Wrobel, S. Bała, M. Czyzycki, M. Golasik, T. Librowski, B. Ostachowicz, W. Piekoszewski, A. Surówka, M. Lankosz, Combined micro-XRF and TXRF methodology for quantitative elemental imaging of tissue samples, Talanta 162 (2017) 654–659.
[20] E.A. Hughes, S.C. Cox, M.E. Cooke, O.G. Davies, R.L. Williams, T.J. Hall, L.M. Grover, Interfacial Mineral Fusion and Tubule Entanglement as a Means to Harden a Bone Augmentation Material, 2018.
[21] N. Zoeger, P. Roschger, J.G. Hofstaetter, C. Jokubonis, G. Pepponi, G. Falkenberg, P. Fratzl, A. Berzlanovich, W. Osterode, C. Streli, P. Wobrauschek, Lead accumulation in tidemark of articular cartilage, Osteoarthritis Cartilage 14 (2006) 906–913.
[22] G. Sohár, E. Pallagi, P. Szabó-Révész, K. Tóth, New thermogravimetric protocol for the investigation of normal and damaged human hyaline cartilage, J. Therm. Anal. Calorim. 89 (2007) 853–856.
[23] G.M. Brouwer, A.W. Van Tol, A.P. Bergink, J.N. Belo, R.M. Bernsen, M. Reijman, H.A. Pols, S.M. Bierma-Zeinstra, Association between valgus and varus alignment and the development and progression of radiographic osteoarthritis of the knee, Arthritis Rheum. 56 (2007) 1204–1211.
[24] R. Moyer, W. Wirth, J. Duryea, F. Eckstein, Anatomical alignment, but not goniometry, predicts femorotibial cartilage loss as well as mechanical alignment: data from the osteoarthritis initiative, Osteoarthritis Cartilage 24 (2016) 254–261.
[25] D. Kumar, K.T. Manal, K.S. Rudolph, Knee joint loading during gait in healthy controls and individuals with knee osteoarthritis, Osteoarthritis Cartilage 2111 (2013).
[26] M. Szarko, K. Muldrew, J.E. Bertram, Freeze-thaw treatment effects on the dynamic mechanical properties of articular cartilage, BMC Musculoskeletal Disorders 11 (2010) 231.
[27] G.R. Fulcher, D.W.L. Hukins, D.E.T. Shepherd, Viscoelastic properties of bovine articular cartilage attached to subchondral bone at high frequencies, BMC Musculoskeletal Disorders 10 (2009).
[28] D.M. Espino, D.E.T. Shepherd, D.W.L. Hukins, Viscoelastic properties of bovine knee joint articular cartilage: dependency on thickness and loading frequency, BMC Musculoskeletal Disorders 15 (2014) 205.
[29] D.K. Temple, A.A. Cederlund, B.M. Lawless, R.M. Aspden, D.M. Espino, Viscoelastic properties of human and bovine articular cartilage: a comparison of frequency-dependent trends, BMC Musculoskeletal Disorders 17 (419) (2016).
[30] B. Pearson, D.M. Espino, Effect of hydration on the frequency-dependent viscoelastic properties of articular cartilage, Proc. Inst. Mech. Eng., Part H 227 (2013) 1246–1252.
[31] J.Q. Yao, B.B. Seedhom, Mechanical conditioning of articular cartilage to prevalent stresses, Br. J. Rheumatol. 32 (1993) 956–965.
[32] T. McCormack, J.M. Mansour, Reduction in tensile strength of cartilage precedes surface damage under repeated compressive loading in vitro, J. Biomech. 31 (1998) 55–61.
[33] A. Verteramo, B.B. Seedhom, Effect of a single impact loading on the structure and mechanical properties of articular cartilage, J. Biomech. 40 (2007) 3580–3589.
[34] B.M. Lawless, S.C. Barnes, D.M. Espino, D.E. Shepherd, Viscoelastic properties of a spinal posterior dynamic stabilisation device, J. Mech. Behav. Biomed. Mater. 59 (2016) 519–526.
[35] D.E.T. Shepherd, B.B. Seedhom, Thickness of human articular cartilage in joints of the lower limb, Ann. Rheum. Dis. 58 (1999) 27–34.
[36] E. Radin, K. Yang, C. Riegger, V. Kish, J. O'Connor, Relationship between lower limb dynamics and knee joint pain, J. Orthop. Res. 9 (1991) 398–405.
[37] R.A. Bank, M. Soudry, A. Maroudas, J. Mizrahi, J.M. Tekoppele, The increased swelling and instantaneous deformation of osteoarthritic cartilage is highly correlated with collagen degradation, Arthritis Rheum. 43 (2000) 2202–2210.
[38] P.J. Basser, R. Schneiderman, R.A. Bank, E. Wachtel, A. Maroudas, Mechanical properties of the collagen network in human articular cartilage as measured by osmotic stress technique, Arch. Biochem. Biophys. 351 (1998) 207–219.
[39] M.D. Crema, D.J. Hunter, D. Burnstein, F.W. Roemer, L. Li, F. Eckstein, N. Krishnan, M.-P.H. Le-Graverand, A. Guermazi, Association of changes in delayed gadolinium-enhanced MRI of cartilage (dGEMRIC) with changes in cartilage thickness in the medial tibiofemoral compartment of the knee: a 2 year follow-up study using 3.0 T MRI, Ann. Rheumatic Diseases 73 (2014) 1935–1941.
[40] A.D. Pearle, R.F. Warren, S.A. Rodeo, Basic science of articular cartilage and osteoarthritis, 2005.
[41] M. Fuerst, O. Niggemeyer, L. Lammers, F. Schäfer, C. Lohmann, W. Rüther, Articular cartilage mineralization in osteoarthritis of the hip, BMC Musculoskeletal Disorders 10 (2009) 166.
[42] H. Sadeghi, B. Lawless, D. Espino, D. Shepherd, Effect of frequency on crack growth in articular cartilage, J. Mech. Behav. Biomed. Mater. 77 (2018) 40–46.
[43] C.T. Chen, M. Bhargava, P.M. Lin, P.A. Torzilli, Time, stress, and location dependent chondrocyte death and collagen damage in cyclically loaded articular cartilage, J. Orthop. Res. 21 (2003) 888–898.
[44] E. Lucchinetti, C.S. Adams, W.E. Horton, P.A. Torzilli, Cartilage viability after repetitive loading: a preliminary report, Osteoarthritis Cartilage 10 (2002) 71–81.
[45] S. Graindorge, W. Ferrandez, E. Ingham, Z. Jin, P. Twigg, J. Fisher, The role of the surface amorphous layer of articular cartilage in joint lubrication, Proc. Inst. Mech. Eng., Part H 220 (2006) 597–607.
[46] F. Nelson, L. Dahlberg, S. Laverty, A. Reiner, I. Pidoux, M. Ionescu, G.L. Fraser, E. Brooks, M. Tanzer, L.C. Rosenberg, P. Dieppe, A. Robin Poole, Evidence for altered synthesis of type II collagen in patients with osteoarthritis, J. Clin. Invest. 102 (1998) 2115–2125.
[47] M. Nickien, A. Thambyah, N.D. Broom, How a decreased fibrillar interconnectivity influences stiffness and swelling properties during early cartilage degeneration, J. Mech. Behav. Biomed. Mater. 75 (2017) 390–398.
[48] F. Guilak, Biomechanical factors in osteoarthritis, Best Pract. Res.: Clin. Rheumatol. 25 (2011) 815–823.
[49] J. Sanchez-Adams, H.A. Leddy, A.L. McNulty, C.J. O'Conor, F. Guilak, The mechanobiology of articular cartilage: bearing the burden of osteoarthritis, Curr. Rheumatol. Rep. 16 (2014) 451.
[50] F. Guilak, B. Fermor, F.J. Keefe, V.B. Kraus, S.A. Olson, D.S. Pisetsky, L.A. Setton, J. B. Weinberg, The role of biomechanics and inflammation in cartilage injury and repair, Clin. Orthopaedics Related Res. (2004) 17–26.
[51] A.M. Philp, R.L. Collier, L.M. Grover, E.T. Davis, S.W. Jones, Resistin promotes the abnormal Type I collagen phenotype of subchondral bone in obese patients with end stage hip osteoarthritis, Sci. Rep. 7 (2017) 4042.
[52] M.J. Pearson, D. Herndler-Brandstetter, M.A. Tariq, T.A. Nicholson, A.M. Philp, H.L. Smith, E.T. Davis, S.W. Jones, J.M. Lord, IL-6 secretion in osteoarthritis patients is mediated by chondrocyte-synovial fibroblast cross-talk and is enhanced by obesity, Sci. Rep. 7 (2017) 3451.